CROATICA CHEMICA ACTA CCACAA **69** (2) 689–708 (1996)

ISSN-0011-1643
CCA–2335

Original Scientific Paper

Self-aggregation of α,ω-Alkanediols into Two and Three Dimensional Crystallites at the Air-Water Interface. Relevance to Ice Nucleation*

Ronit Popovitz-Biro,[a] *Ron Edgar,*[a] *Jaroslaw Majewski,*[a] *Sidney Cohen,*[a] *Lev Margulis,*[a] *Kristian Kjaer,*[b] *Jens Als-Nielsen,*[b] *Leslie Leiserowitz,*[a] *and Meir Lahav*[a]

[a]*Department of Materials and Interfaces, The Weizmann Institute of Science, 76100 Rehovot, Israel*

[b]*Department of Physics, Riso National Laboratory, DK-4000 Roskilde, Denmark*

Received January 31, 1996; accepted April 10, 1996

A correlation is presented between the crystalline structure of monolayers and multilayers of α,ω-alkanediols HO-$(CH_2)_n$-OH (n = 16, 18, 19, 21, 22, 23, 24, 30) at the air-water interface and their function as ice nucleators. Structural elucidation was carried out by the following methods: grazing incidence X-ray diffraction, scanning force microscopy, cryo-transmission electron microscopy and external reflection Fourier transform-infrared spectroscopy.

INTRODUCTION

In previous studies on induced ice nucleation by monolayers of aliphatic alcohols, we observed that nucleation is extremely sensitive to the molecular structure and packing arrangement of the monolayer.[1] Following the above investigations, it seemed that monolayers of α,ω-alkanediols HO-$(CH_2)_n$-OH should be candidates to test for ice nucleation behavior and to correlate their nucleation efficiency with the structures at the air-water interface. It has been an accepted model, based on pressure-area isotherms, that single chain double headed amphiphiles, or bolaamphiphiles, when spread on water, lie flat on the surface and, upon compression, adopt a bent conformation with

* This paper is dedicated with great admiration to Vlado Prelog on the occasion of his ninetieth birthday.

the polar groups anchored at the water and the hydrocarbon chain looped vertically.[2,3] According to this model, such monolayers should be poor ice nucleators due to disordered arrangement of the chains and possible complexity of several coexisting conformations. We found unexpectedly, that spreading the α,ω-alkanediols on water drops induced freezing in a temperature range similar to that of the aliphatic monoalcohols. This observation triggered a systematic study on a series of α,ω-alkanediols of various chain lengths using modern analytical tools such as external reflection Fourier transform infrared (FT-IR), grazing incidence X-ray diffraction (GID),[4] X-ray reflectivity, cryo-transmission electron microscopy (cryo-TEM) and scanning force microscopy (SFM).[5]

EXPERIMENTAL SECTION

Ice nucleation experiments were carried out in a set up and according to the procedure described in Ref. 1.

Pressure-Area Isotherms were measured on a computer-controlled Lauda filmbalance, placed in a laminar hood and thermostated to 20 °C. Spreading solutions of 5×10^{-4} M were prepared in $CHCl_3$ (Merck, analytical grade). The water used was purified by a Millipore purification system to give a resistivity of 18 MW.

FT-IR Measurements of the monolayers on the water surface were carried out by a commercial Specac monolayer accesory, modified to enable thermostating of the subphase. The angle of incidence was 25° from the normal to the surface. Reflection-absorption spectra were obtained by ratioing the single beam monolayer spectrum on water against the single beam reflectance spectrum of pure water. Each spectrum was a result of coaddition of 4000 scans at resolution of 2 cm^{-1}. Spectra were obtained on a Bruker IFS66.

Cryo-TEM Measurements. Samples were prepared on collodion-carbon coated-400 mesh, bare 1000 mesh or plastic holey EM grids.[6] The grids were placed on a stainless steel mesh which was immersed in the water in a specially designed Teflon trough.[7] Monolayers were spread on the water surface at 20 °C, after which the subphase was cooled to 5 °C and the water was slowly drained by a motor-driven syringe. The grids with the deposited monolayers were mounted on a plunging device, the excess of water was blotted by filter paper and the grids were rapidly plunged into liquid ethane to form vitreous ice. The specimens were loaded into a Gatan 626 cold stage and examined in a Philips CM12 transmission electron microscope operated at 100 kV. The samples were maintained at –175 °C during examination and diffraction measuremts. Bright field imaging were obtained after sublimation of vitreous ice by raising the temperature to –90 °C and cooling back to –175 °C inside the electron microscope column.

SFM Measurements. Samples were prepared by the same horizontal transfer technique as used for deposition on the EM grids. Freshly cleaved mica was placed onto the stainless steel mesh in the subphase before spreading the monolayer. After thermal equilibration was reached the water level was lowered by slow draining with a motor-driven syringe. SFM measurements were made in air using a Topo-

metrix TMX 2010 stage. Integrated Si_3N_4 pyramidal tips, on cantilevers with force constants between 0.03–0.4 N/m were used. Contact forces of 2–5 nN above the equilibrium force (signal recorded before contact made) were applied during imaging.

Materials. 12-Hydroxydodecanoic acid, 16-hydroxyhexadecanoic acid, tetracosanedioic acid used as starting materials for synthesis were purchased from Aldrich and heptanedioic acid and nonanedioic acid from Fluka.

Synthesis of α,ω-Alkanediols. Alkanediols with n = 18, 21, 22, 23, and 30 were synthesized *via* Kolbe electrolysis.[8] Diols with n = 18, 22 and 30 were prepared *via* symmetric coupling of monomethyl ester of decanedioic acid, 12-hydroxydodecanoic acid and 16-hydroxyhexadecanoic acid respectively. Alkanediols with n = 21 and 23 were synthesized by cross coupling of 16-hydroxyhexadecanoic acid with monomethyl ester of heptanedioic acid and nonanedioic acid respectively. The resulting monomethyl or dimethyl esters were further reduced to the diols by $LiAlH_4$.

Alkanediols with n = 16 and 24 were prepared by reducing the methyl ester of 16-hydroxyhexadecanoic acid and dimethyl ester of tetracosanedioic acid respectively by $LiAlH_4$. All products were purified by column chromatography on silica gel using 5% ethanol in CH_2Cl_2 as eluent. Products were analyzed by GC-MS, NMR and IR spectroscopy.

RESULTS

Ice Nucleation

The ice nucleation efficiencies of the various α,ω-alkanediols HO-$(CH_2)_n$-OH films were determined by measuring the threshold freezing temperatures of supercooled water drops covered by these at a surface area of 20 Å^2 per molecule (assuming monolayer formation). The results are compared with the freezing temperatures induced by the corresponding monoalcohols,[1] as shown in Table I. As in the series of aliphatic alcohols, an odd-even effect

TABLE I

Freezing temperatures of supercooled water drops covered by aliphatic alcohols and by alkanediols

n	$CH_3(CH_2)_nOH$	$HO(CH_2)_nOH$
16	−13.7 ± 0.5	−6.2 ± 0.6
18	−10.9 ± 1.0	−5.8 ± 0.4
19	−7.2 ± 0.6	−8.2 ± 0.8
21	−5.3 ± 1.0	−8.0 ± 0.7
22	−7.9 ± 0.5	−5.7 ± 0.8
23	−3.6 ± 0.7	−9.5 ± 0.9
24	−7.0 ± 0.6	−4.7 ± 0.5
30	−7.5 ± 0.5	−4.7 ± 0.4

was observed; however in the alkanediol series, molecules with n = even nucleate ice at higher temperatures than those with n = odd. For n = even the nucleation induced by the diols is at higher temperatures than those obtained by the corresponding monoalcohols, the largest difference observed is for n = 16. For n = odd, ice nucleation occurred at lower temperatures than that obtained by the corresponding monoalcohols. In contrast to the behavior observed in the aliphatic alcohol series, the influence of alkanediol chain length on nucleation efficiency is minor.

Pressure-Area Isotherms

Pressure-area isotherms of the α,ω-alkanediols HO-$(CH_2)_n$-OH n = 16, 18, 19, 21, 22, 23, 24, 30 have been measured, of which some examples are shown in Figure 1. For alkanediols with n = 16, 18, 21, 22, 24 the apparent areas per molecule obtained were in the range of 10–14 Å^2, which is lower than that of the corresponding aliphatic monoalcohols (19–20 Å^2) and much lower than the area expected for the molecules in a bent conformation. For alkanediols with n = 16, 18 and 19 a plateau region of constant pressure was obtained starting at 65 Å^2, 100 Å^2 and 80 Å^2 respectively followed by a steep rise in pressure at about 14–15 Å^2. The isotherms of alkanediols with n = 23 and 30 were more expanded with areas per molecule of 20 and 23 Å^2 respectively.

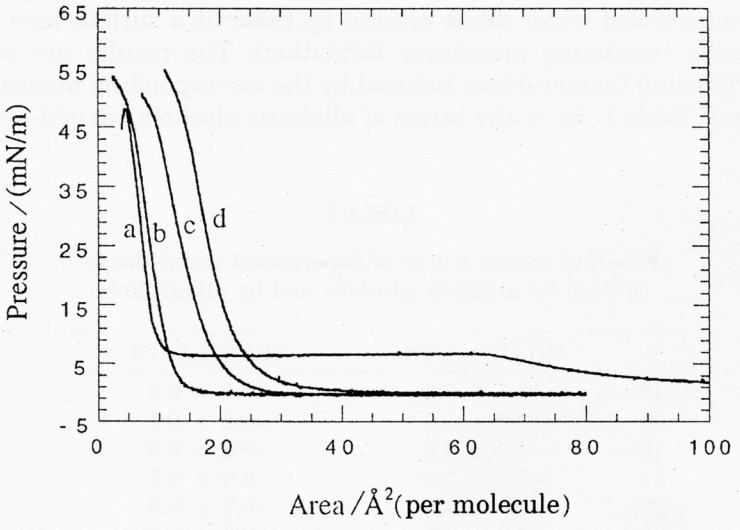

Figure 1. Pressure-area isotherms of α,ω-alkanediols HO-$(CH_2)_n$-OH , (a) n = 16, (b) n = 24, (c) n = 23 and (d) n = 30 at 20 °C.

External Reflection FT-IR

External reflection FT-IR has been used to measure the vibrational spectra of films in this α,ω-alkanediol series. The antisymmetric and symmetric methylene stretching frequencies are known to be conformational sensitive and can be correlated with the degree of order in the hydrocarbon chain.[9,10] Measurements were made on these films *in situ* at the air-water interface, at 20 °C and at surface areas of 60, 30 and 20 Å^2 per molecule. The spectra obtained for HO-$(CH_2)_n$-OH with n = 21, 22, 23, 24, 30 were very similar and thus only the spectra for n = 24 are shown in Figure 2. With a decrease in average area per molecule upon compression, no shift in the frequencies was observed, only an increase in band intensities of the antisymmetric and symmetric CH_2 stretching vibrations at 2917 and 2848 cm^{-1}. This behavior indicates increase in the number of molecules per area but no change in order upon compression of the film, suggesting that even at 30% surface coverage the molecules are arranged in a highly ordered phase as characterized

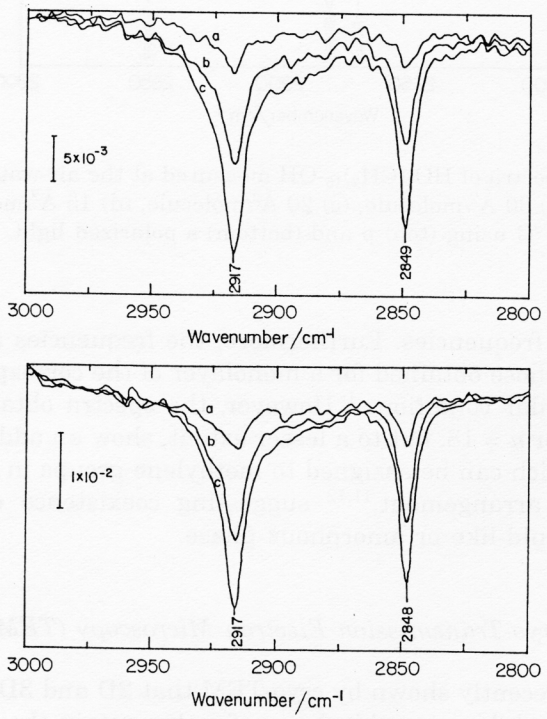

Figure 2. FT-IR spectra of HO-$(CH_2)_{24}$-OH measured at the air-water interface at (a) 60 Å^2/molecule, (b) 30 Å^2/molecule and (c) 20 Å^2/molecule at 20 °C using (top) p and (bottom) s polarized light.

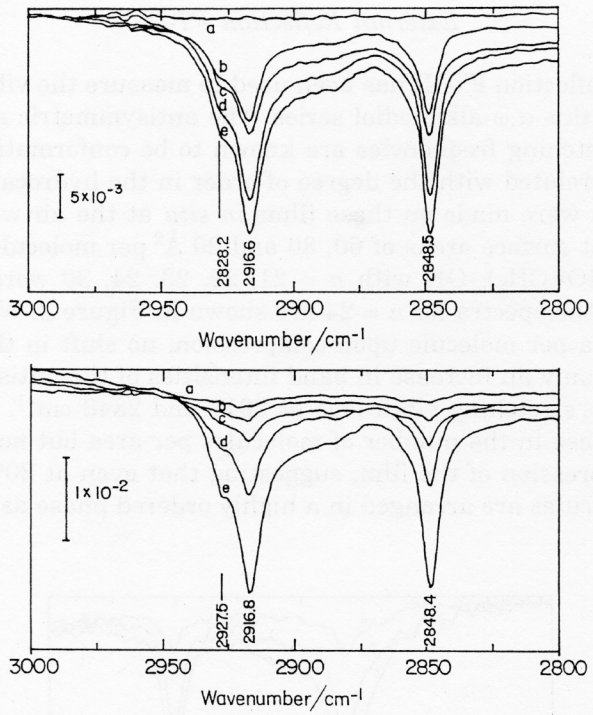

Figure 3. FT-IR spectra of HO-$(CH_2)_{16}$-OH measured at the air-water interface at (a) 60 Å^2/molecule, (b) 30 Å^2/molecule, (c) 20 Å^2/molecule, (d) 15 Å^2/molecule and (e) 10 Å^2/molecule at 20 °C using (top) p and (bottom) s polarized light.

by the observed frequencies. Furthermore, the frequencies and bandwidths were similar to those obtained for a monolayer of the corresponding monoalcohol under similar conditions.[1] However, the spectra obtained for n = 16 (Figure 3) and for n = 18, but to a lesser extent, show an additional shoulder at 2928 cm^{-1} which can be assigned to methylene groups in a conformationally disordered arrangement,[11,12] suggesting coexistence of a crystalline phase with a liquid-like or amorphous phase.

Cryo-Transmission Electron Microscopy (TEM)

It has been recently shown by cryo-TEM that 2D and 3D self-aggregates of various amphiphiles on a thin layer of water, retain their crystalline integrity following fast vitrification of the water subphase.[7] This series of α,ω-alkanediols was also studied by cryo-TEM, a method which allows structural characterization of the films using both diffraction and imaging modes. The

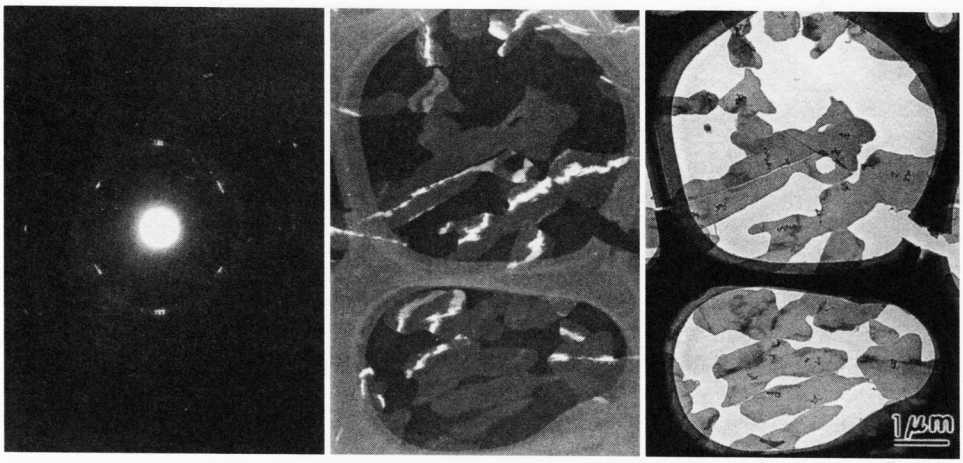

Figure 4. (left) Electron diffraction pattern of HO-$(CH_2)_{16}$-OH crystallites on vitreous ice, (center) dark-field image and (right) bright field image of the crystallites on plastic holey EM grids after sublimation of ice.

α,ω-alkanediols were spread on water at 20 °C, to an average area per molecule of 20 Å^2 (assuming monolayer formation) and the samples were prepared according to a previously described method.[13] Figures 4 and 5 show electron diffraction patterns, bright and dark field images of alkanediols

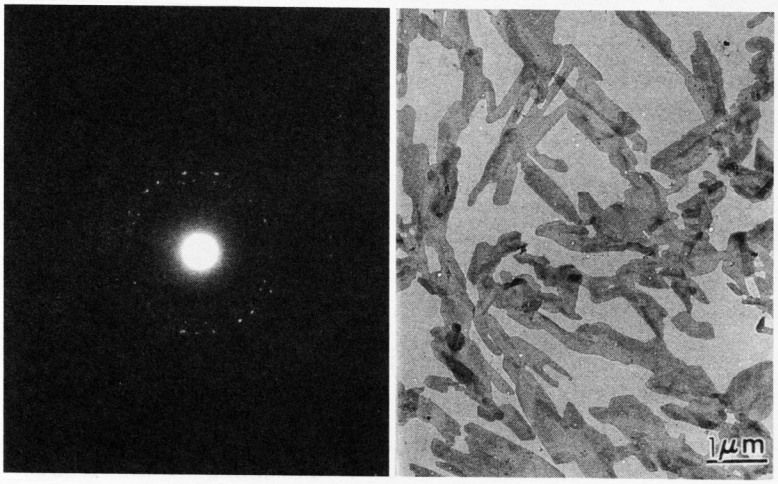

Figure 5. (left) Electron diffraction pattern of HO-$(CH_2)_{24}$-OH crystallites on vitreous ice and (right) bright field image of the crystallites on plastic coated EM grids after sublimation of ice.

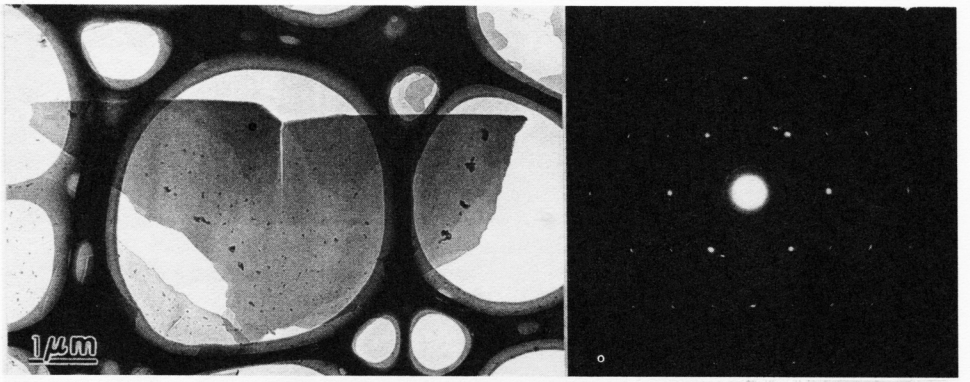

Figure 6. (left) Bright field image of crystallites of HO-$(CH_2)_{18}$-OH on holey EM grids and (right) single crystal diffraction pattern obtained from the above crystallite after sublimation of vitreous ice.

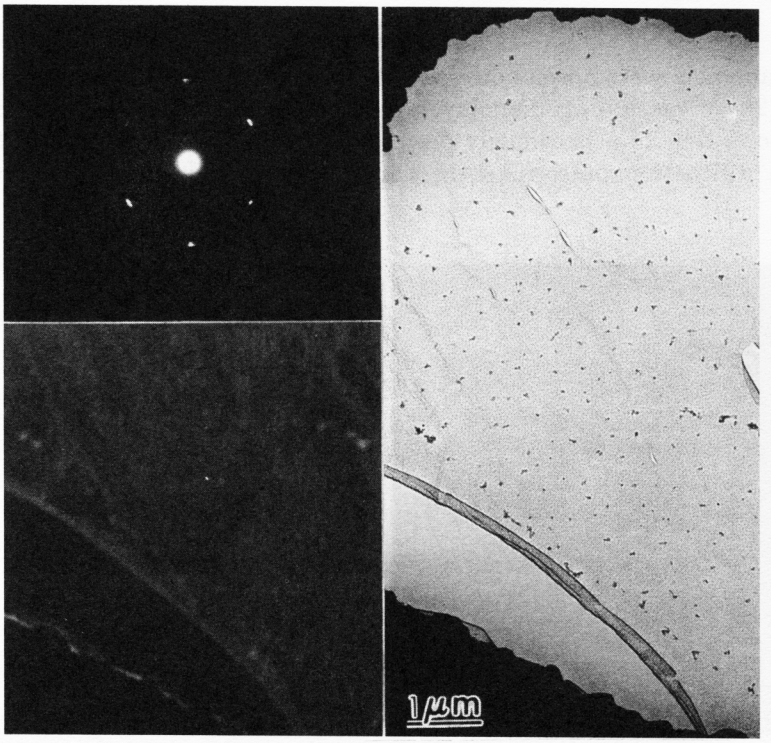

Figure 7. (left top) Electron diffraction pattern of a film of HO-$(CH_2)_{21}$-OH, (left bottom) dark field image and (right) bright field image of the above film on a 1000 mesh bare grid, after sublimation of ice.

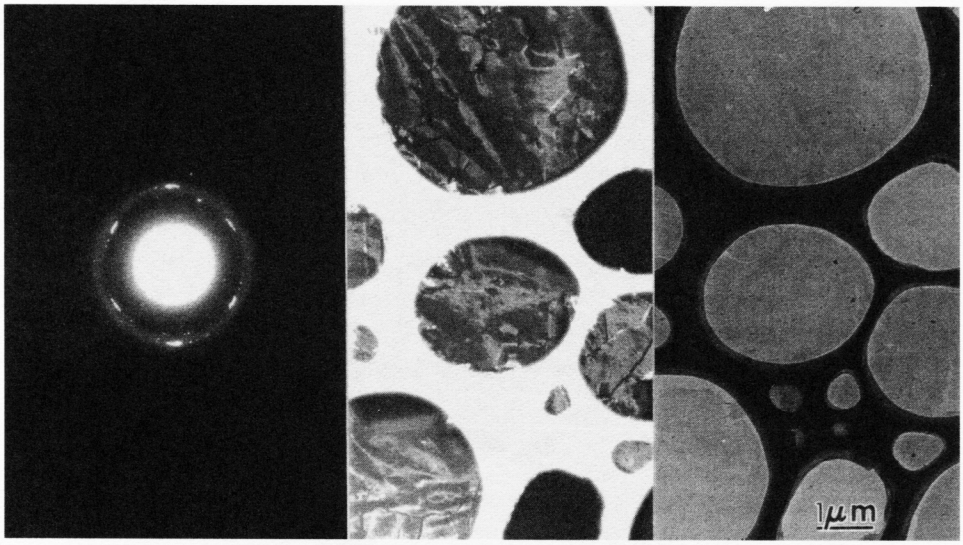

Figure 8. (left) Electron diffraction pattern of a film of HO-$(CH_2)_{23}$-OH on vitreous ice, (center) dark field image and (right) bright field image of the above film after sublimation of ice. Note that the dark areas in the bright field image are due to the plastic support creating the holey grid and the freely suspended monolayer is observed inside the holes.

with n = 16 and 24. Single crystal diffraction patterns, obtained either on vitreous ice or after its sublimation, showed three characteristic d spacings of 4.2, 3.7 and 2.5 Å whose $\{h,k\}$ indices were assigned as $\{1,1\}$, $\{0,2\}$ and $\{2,0\}$, yielding a rectangular cell a = 5.0 and b = 7.4 Å. These cell dimensions provide fingerprint evidence for a herringbone arrangement of the hydrocarbon chains in the orthogonal $O_\perp$ motif.[14] Bright and dark field images revealed elongated plate-like crystallites of length 1–5 μm, similar to those observed[5] for alkanediol with n = 22. Bright field images of alkanediol with n = 18 show plate-like crystallites 5–10 μm in size, yielding single crystal diffraction patterns with a large number of high order reflections (Figure 6). The alkanediols with n = 21, 23 and 30, showed similar diffraction patterns, either from single crystals or several slightly misaligned crystals, but with lower intensities and higher sensitivity to the electron beam. However, bright or dark field images from these alkanediols, obtained after sublimation of vitreous ice, revealed continuous membrane-like films with holes, foldings and defects (Figure 7, 8, 9), reminiscent of images that were previously obtained from other amphiphiles that form monolayers.[7,13,15] Thus, it seems that the number of methylene groups in the alkanediol chain has an influence on the tendency to spontaneously form either monolayer or multilayer crystallites, when spread on the water surface.

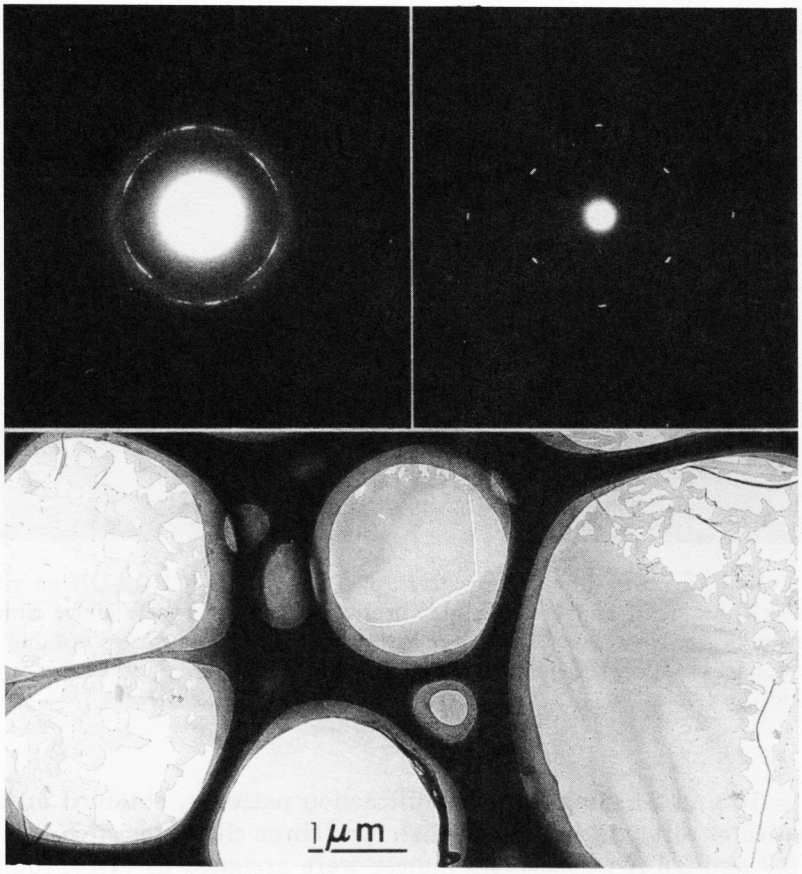

Figure 9. (top left) Electron diffraction pattern of a film of HO-$(CH_2)_{30}$-OH on vitreous ice, (top right) single crystal electron diffraction pattern obtained from a selected area of the above film and (bottom) bright field image after sublimation of ice.

Scanning Force Microscopy (SFM)

SFM is a tool for studying surface phenomena from nanometer to micron scale and has been used to study the structures and morphologies of transferred monolayers and Langmuir Blodgett multilayers on solid supports.[16–19] Here we applied this technique to investigate the surface topography and layer thickness of the films of α,ω-alkanediols deposited on freshly cleaved mica. Figure 10 shows the SFM image and height analysis for a film of alkanediol with n = 16 spread on water to 20 Å^2 per molecule and transferred onto mica. Similar to the images obtained by electron microscopy, elongated crystallites of a few microns in length were observed. Cross sectional profile

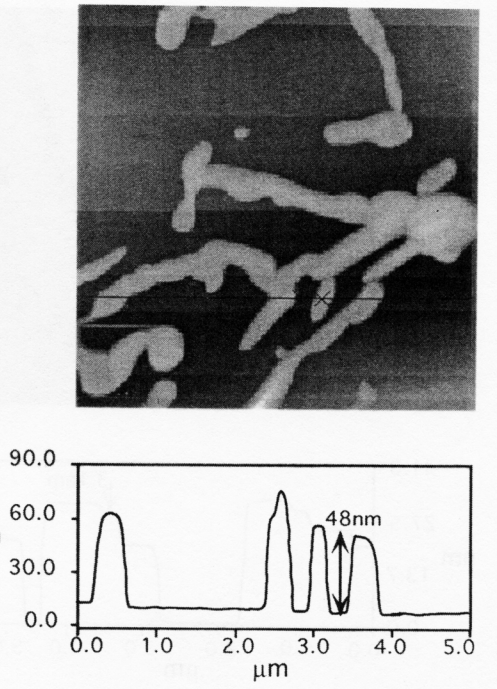

Figure 10. A 5 μm × 5 μm SFM image and height profile along the indicated line of HO-$(CH_2)_{16}$-OH crystallites on freshly cleaved mica; crystallite thickness is given by the vertical arrow in the profile.

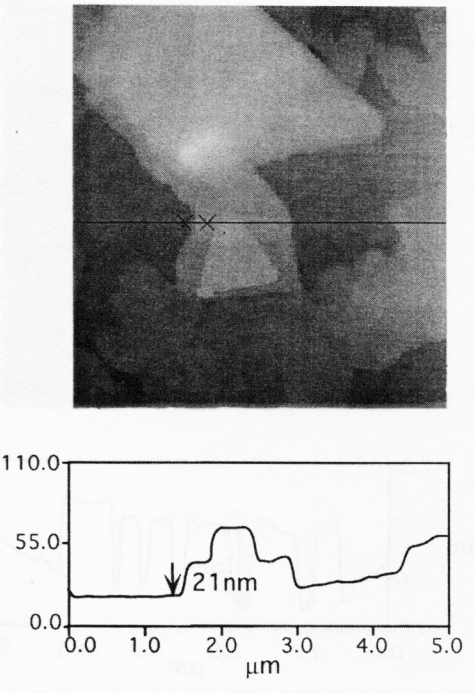

Figure 11. A 5 μm × 5 μm SFM image and height profile along the indicated line of HO-$(CH_2)_{18}$-OH crystallites on freshly cleaved mica.

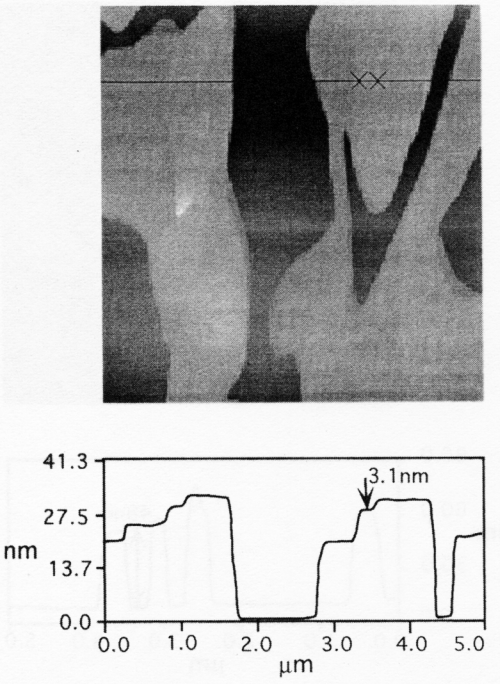

Figure 12. A 5 μm × 5 μm SFM image and height profile along the indicated line of HO-$(CH_2)_{24}$-OH crystallites on freshly cleaved mica; a step of monolayer thickness is given by the vertical arrow in the profile.

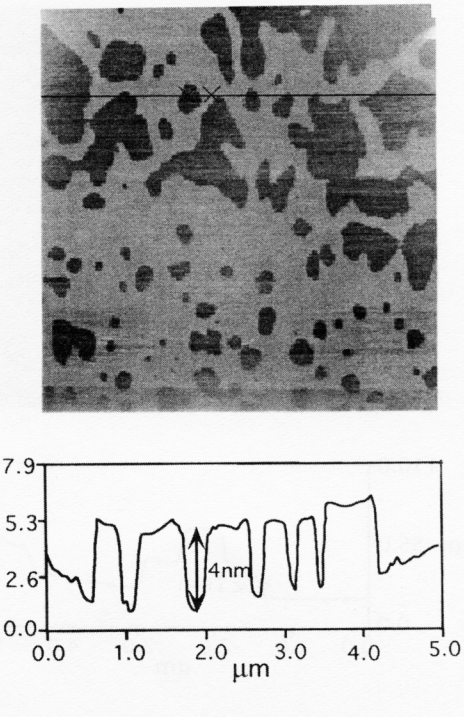

Figure 13. A 5 μm × 5 μm SFM image and height profile along the indicated line of a monolayer of HO-$(CH_2)_{30}$-OH deposited on freshly cleaved mica. The monolayer thickness is given by the vertical arrow in the profile.

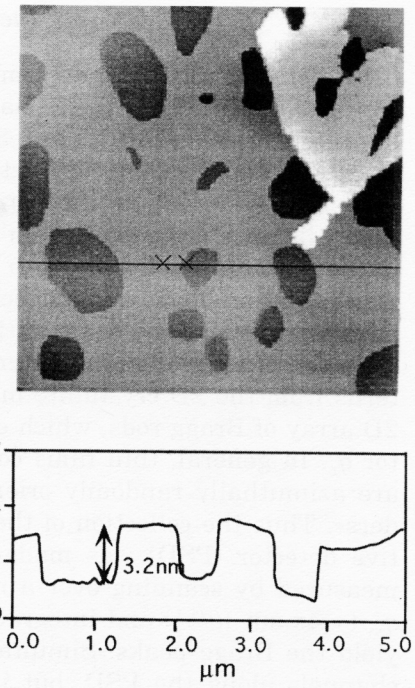

Figure 14. A 5 μm × 5 μm SFM image and height profile along the indicated line of a film of HO-$(CH_2)_{23}$-OH deposited on freshly cleaved mica. Thickness given by the vertical arrow in the profile corresponds to a monolayer and the bright area on the right corner is of bilayer thickness (not shown in profile).

through several crystallites revealed thicknesses of 24–64 nm corresponding to 10–30 molecular layers, assuming that the molecules are aligned perpendicular to the layer plane. For alkanediol with n = 18, large areas of the support were covered by films 3–4 layers thick showing steps of molecular length. Occasionally, triangular-shaped crystals 20–40 nm thick which correspond to 8–16 layers, were also observed as shown in Figure 11. Elongated plate-like crystallites of 1–5 μm size and with similar morphologies to those obtained for n = 16 were observed from alkanediol with n = 24. However, cross sections through these crystallites yielded 4–10 molecular layers and steps of 3.2 nm, corresponding to a monolayer (Figure 12). Scanning of deposited films from alkanediols with n = 23 and 30 resulted in different topographic pictures than the previous systems. Continuous membrane-like films with holes of various shapes, were observed for the diol with n = 30 (Figure 13), in agreement with the electron microscopy images. Surface topography across the holes revealed film thickness of 4.0 nm which corresponds to the calculated molecular length in an all-*trans* extended conformation. Similarly, large areas covered by a monolayer (thickness of 3.2 nm) with holes was observed from samples of alkanediol with n = 23 (Figure 14). In addition to the monolayer, regions of bilayers were also observed.

Grazing Incidence X-ray Diffraction

A detailed structure determination of the multilayer formed by α,ω-docosanediol n = 22 on water has been reported.[4] Here we describe the alkanediol series n = 16, 23 and 30. The GID measurements were carried out using the liquid surface diffractometer on beamline BW1 at Hasylab DESY, Hamburg. A sealed and thermostated Langmuir trough equipped with a Wilhelmy balance was mounted on the diffractometer. The films were measured in the uncompressed state with no detectable surface pressure. The synchrotron radiation beam was monochromated to a wavelength of λ = 1.35 Å and adjusted to strike the water surface at an incident angle of $\alpha = 0.85\ \alpha_c$ where α_c is the critical angle of water for total external reflection. The GID patterns from the 2D crystallite monolayers on the water surface arise from a 2D array of Bragg rods, which extend parallel to the vertical scattering vector q_z. In general, thin films composed of crystallites on the water surface are azimuthally randomly oriented and so may be described as »2D powders«. Thus the collection of the diffracted radiation using a position sensitive detector (PSD) was made in two ways. The scattered intensity was measured by scanning over a range along the horizontal scattering vector q_{xy} (= $4\pi \sin\{\theta/\lambda\}$) and integrated over the whole q_z window of the PSD, to yield the Bragg peaks. Simultaneously, the scattered intensity recorded in channels along the PSD, but integrated over the scattering vector in the horizontal plane across a Bragg peak, produced q_z resolved scans called Bragg rod profiles. The information extracted from measured profiles include the angular position (2θ) of the Bragg peaks which yield the repeat distances $d = 2\pi / q_{xy}$ for the 2D lattice structure. The Bragg peaks may be indexed by two Miller indices h, k to yield the unit cell. The full width at half maximum (FWHM) of the Bragg peak in q_{xy} units yields the 2D crystalline coherence length associated with the h, k reflection. The intensity at a particular value of q_z in a Bragg rod is determined by the square of the molecular structure factor $|F_{h,k(qz)}|$ (for further details see Refs. 20 and 21). The variation of intensity I_{hk} along the Bragg rod as a function of q_z (*i.e.* the Bragg rod profile), may provide precise information on the molecular chain packing by applying rigid body refinement for an atomic molecular model.

In this series of alkanediols two intense Bragg peaks were observed at $q_{xy} \approx 1.5$ and 1.7 Å^{-1} which lead to a rectangular cell, $a \approx 5.0$ Å and $b \approx 7.3$ Å so that the two reflections are indexed as {1,1} and {0,2} respectively. These cell dimensions are finger-print evidence of a herringbone motif of the hydrocarbon chains, generated by glide symmetry in the unit cell.

The alkanediol with n = 16 was measured at 100–300% surface coverage assuming monolayer formation. The GID patterns differ in intensity and hence the number of observed Bragg rods are proportional to the amount of material. The molecules are packed in a rectangular cell with dimensions a = 5.09 Å, b = 7.20 Å. At 300% surface coverage, the GID pattern consists

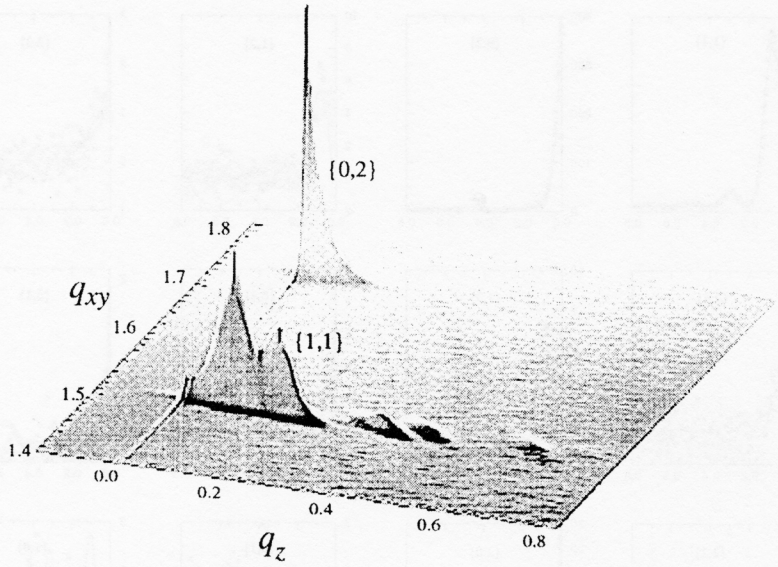

Figure 15. Two dimensional intensity distribution $I(q_{xy},q_z)$ of the diffraction pattern of the C_{16} diol on the water surface. The {1,1} and {0,2} Bragg rods are shown.

of nine observed Bragg rods (Figure 15) with film thickness corresponding to 5–10 layers. The {0,2} reflection peaks at $q_z \approx 0$ Å^{-1} and the {2,0} peaks at $q_z \approx 0.1$ Å^{-1}, which suggests a minor molecular tilt along the a direction within the layer. This tilt normally indicates an a-glide symmetry, in the herringbone motif. However, there is a weak, yet well structured {1,0} reflection including distinct intensity modulations. A true a-glide would render the {1,0} reflection symmetry forbidden. To account for this apparent inconsistency, the glide plane must be relaxed. A satisfactory model, one which fits all the observed Bragg rods with respect to each intensity profile and a correct distribution of the overall intensity, was not found. None the less, the intense low order reflections do indicate a pseudo glide packing with a 1.5° molecular tilt along the a direction. Contrary to the three dimensional crystal structure,[22] in which the molecules within the layer are related by translation and tilted by about 35° with respect to the layer plane, in the film the molecules are aligned almost normal to the water surface in the herringbone motif.

The alkanediol with $n = 30$ was measured at 100% surface coverage and consists primarily of a monolayer and of some multilayer phase. The monolayer (ca. 85% occupancy *vis-a-vis* that of multilayer) phase packs in a rectangular cell with $a = 5.00$ Å, $b = 7.38$ Å. The best model was found for chains tilted by 2.5° along the b axis and leaned by 2° along the a direction corresponding essentially to a $p1g1$ plane group (*i.e.* a primitive cell with the

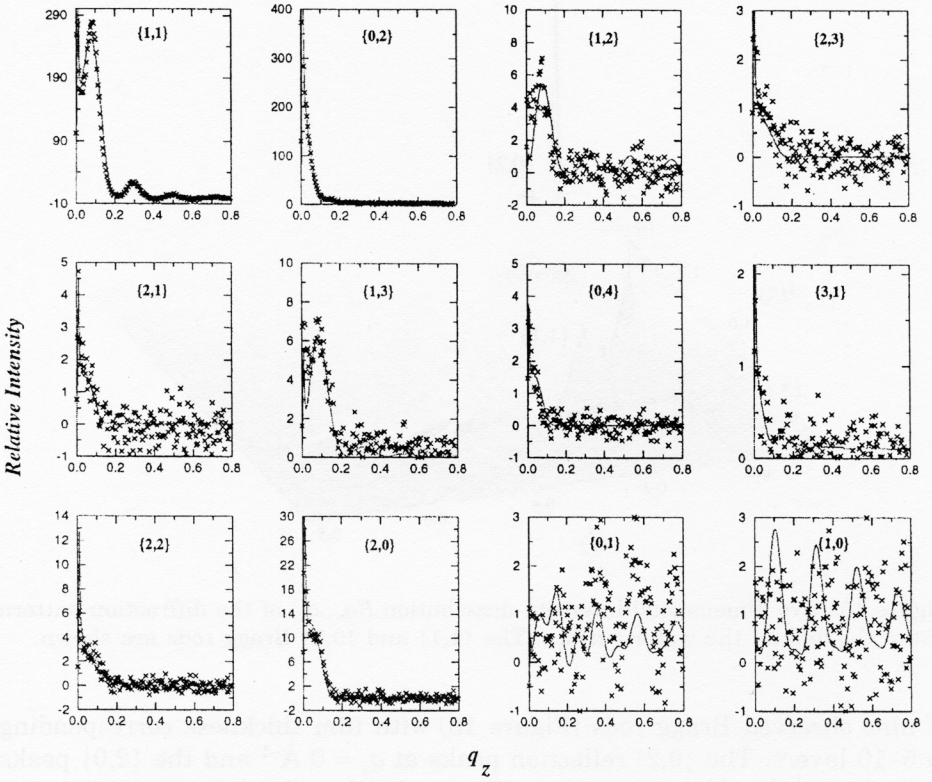

Figure 16. Observed (crosses) and calculated (lines) Bragg rods intensity profiles $I(q_z)$ of the C_{23}-diol bilayer on water.

glide g plane along the b axis) but with the glide somewhat relaxed. The multilayer phase exhibits two reflections peaking at the same q_{xy} value corresponding to a 4.4 Å spacing. Assuming a herringbone motif and the need to satisfy hydrogen bonds we can generate a reasonable model in which the two reflections correspond to the {1,1} at lower q_z value, and {0,2} at high q_z. This assignment yields a 5.1 by 8.8 Å cell and a molecular tilt of 35° along the 8.8 Å axis.

The diffraction pattern of an alkanediol with an odd number of carbons n = 23, consists of twelve reflections which were assigned to a rectangular cell with a = 5.0 Å, b = 7.3 Å. The Bragg rod width corresponds to a film two layers thick. Structure elucidation was aided by the 3D structure of alkanediol with n = 9 which packs in the orthorhombic space group $P2_12_12_1$.[23] In the three dimensional crystal structure, one end of each molecule adopts a $C_\alpha OH$ *gauche* conformation about the C_β-C_α bond and the molecules are

aligned normal with respect to the layer plane. This packing allows formation of both inter and intralayer hydrogen bonds between *gauche* and *trans* end C-OH groups. Figure 16 shows the observed and fitted Bragg rod intensity profiles. The model was constructed by applying a *gauche* conformation to one end of an all *trans* C_{23} diol molecule and generating the intralayer packing by a twofold screw axis parallel to *a*. The two layers are related by a twofold screw axis parallel to the *c* axis of length 30.5 Å. The generated orthorhombic cell contains four symmetry related molecules. To best account for the observed intensity profiles, each molecule in the two layers had to be tilted by 1° along the *ab* diagonal; and the top layer has a partial molecular occupancy of 70% (Figure 17).

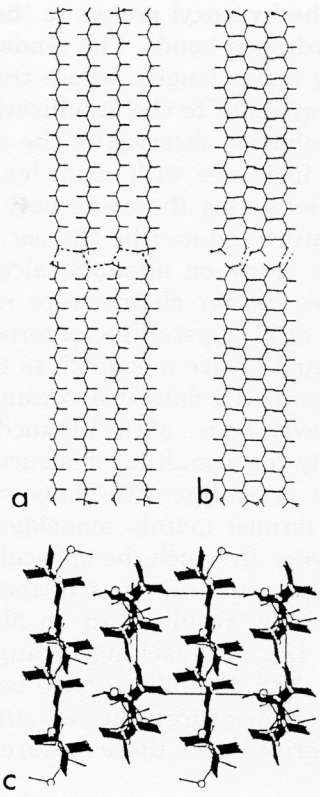

Figure 17. Model packing assignment of the bilayer of the C_{23}-diol on water. (a) (b) (c) views along the *b*, *a*, and *c* axis respectively.

DISCUSSION

In this study ice nucleation measurements and structural elucidation of this series of α,β-alkanediols have been performed in order to obtain a structure-function correlation. Both FT-IR and cryo-TEM measurements strongly suggest that these bolaamphiphiles are self aggregated in highly ordered crystalline phases with the molecules aligned normal to the plane of the mono- or multilayer. SFM measurements showing steps of molecular lengths support this suggestion. For the short molecules $n = 16 - 19$ a coexistence with a less ordered or amorphous phase may be present. The self-aggregation is probably driven by the relatively high energy surface created by the two dimensional (2D) layer of vertically aligned α,ω-alkanediols exposing

one of the hydroxyl groups to the air, leading to multilayers through interlayer hydrogen bonds. The tendency to form multilayers decreases with increasing chain length, where the intralayer methylene-methylene interactions contribute to the stabilization of the monomolecular film. In contrast to the behavior observed in the aliphatic alcohols,[1] whose ice nucleation efficiency increases with chain length for both n = even and n = odd, in the alkanediol series there are only minor differences among the ice freezing temperature induced by the corresponding alkanediols (Figure 18). In our previous study on aliphatic alcohols, the lower freezing temperatures induced by shorter chains were rationalized in terms of a decrease in the amount of 2D crystalline material and a concomitant increase in molecular motion and lattice mismatch to that of ice in terms of unit cell area, as deduced from GID data.[24] According to cryo-TEM and SFM measurements in the n = even series of the alkanediols, the tendency of the molecules to spontaneously form multilayer structures increases with chain shortening. For example, crystallites 10–30 layers thick were obtained with n = 16, whereas n = 30 formed mainly monolayer. Thus, the tendency to form crystalline multilayers, in which the molecular motion is expected to be as in a 3D crystal, cancels out the effect of increasing molecular motion with decreasing chain length, resulting in an almost constant ice nucleation temperature (Figure 18). The packing arrangements of multilayers of the alkanediols (n = 16, 22,[4] 23 and 30) have been determined by grazing incidence X-ray diffraction measurements *in situ* on the water surface. According to the model derived from these mesurements, the molecular chains in an all-*trans*

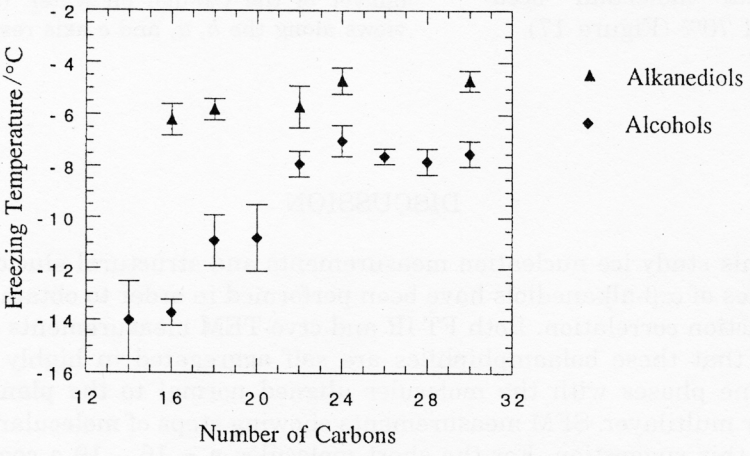

Figure 18. Freezing temperatures of 10 μl supercooled water drops covered by a film of alkanediol HO-$(CH_2)_n$-OH or alcohol $CH_3(CH_2)_n$OH at 20 Å^2/molecule (100% coverage assuming monolayer formation) for n = even as a function n.

conformation are arranged in a herringbone motif and aligned almost perpendicular to the water surface. The layer cell dimensions obtained are a = 5.0 Å, b = 7.3 Å which match well with the ab layer of ice.[24]

It appears that alkanediols in the series with n = odd have a lower tendency to form multilayers than those with n = even. For example, alkanediols with n = 22 and 24 form multilayer crystallites whereas mainly monolayer film was obtained for n = 23. However, for n = 21 there is an inconsistency between the cryo-TEM and the SFM measurements. Cryo-TEM imaging revealed a continuous membrane-like film whereas 2–10 layer thick multilayers were observed by SFM measurements. GID data of this alkanediol could be assigned to 1–2 layers. This specific inconsistency and in general the descrepancy between the number of layers obtained from different techniques, may well result from the fact that these systems deviate from equilibrium. Thus a rearrangement of the monolayer into multilayers may occur during transfer onto the mica support or during sublimation of vitreous ice in the cryo-TEM measurements.

Ice nucleation by alkanediols from the n = odd series is less efficient than by the n = even series. This behavior may be rationalized in terms of the molecular conformation of the odd numbered alkanediols in 3D crystals. In each molecule one of the two C_α-OH bonds adopts a *gauche* conformation about the C_β-C_α bond, such that in a layer *trans* and *gauche* end group conformations alternate. Such arrangement places the oxygen atoms in a lattice which has a poor match to that of ice.[23]

Acknowledgement. – We thank Edna Shavit for the synthesis of the compounds. The project was supported by the Minerva Foundation, Münich, Germany and the Danish Foundation for Natural Sciences. We also acknowledge HASYLAB, DESY, Hamburg for beam time.

REFERENCES

1. R. Popovitz-Biro, J. L. Wang, J. Majewski, E. Shavit, L. Leiserowitz, and M. Lahav, *J. Am. Chem. Soc.* **116** (1994) 1179–1191.
2. M. Ueno, M. Kawanabe, and K. Meguro, *J. Colloid Interface Sci.* **51** (1975) 32–35.
3. P. M. Jeffers and J. Dean, *J. Phys. Chem.* **69** (1965) 2368–2373.
4. J. Majewski, R. Edgar, R. Popovitz-Biro, K. Kjaer, G. W. Bouwman, J. Als-Nielsen, M. Lahav, and L. Leiserowitz, *Angew. Chem., Int. Ed. Engl.* **34** (1995) 649–652.
5. R. Popovitz-Biro, J. Majewski, L. Margulis, S. Cohen, L. Leiserowitz, and M. Lahav, *J. Phys. Chem.* **98** (1994) 4970–4972.
6. A. W. Robards and A. J. Wilson, (Eds.), *Procedures in Electron Microscopy*, John Wiley&Sons, New-York, 1993.
7. J. Majewski, L. Margulis, I. Weissbuch, R. Popovitz-Biro, T. Arad, Y. Talmon, M. Lahav, and L. Leiserowitz, *Advan. Mater.* **7** (1995) 26–35.
8. H. J. Schäfer, *Chemistry and Physics of Lipids*, Elsevier, 1979, Vol. 24, pp 321.

9. R. A. Dluhy and D. G. Cornell, *Fourier Transform Infrared Spectroscopy in Colloid and Interface Science*, Washington DC, 1990, Vol. 447, pp 192.
10. A. Gericke and H. Hühnerfuss, *J. Phys. Chem.* **97** (1993) 12899–12908.
11. R. G. Snyder, H. L. Strauss, and C. A. Elliger, *J. Phys. Chem.* **86** (1982) 5145–5150.
12. D. L. Allara, S. V. Atre, C. A. Ellinger, and R. G. Snyder, *J. Am. Chem. Soc.* **113** (1991) 1852–1854.
13. J. Majewski, L. Margulis, D. Jacquemain, F. Levellier, C. Böhm, T. Arad, Y. Talmon, M. Lahav, and L. Leiserowitz, *Science* **261** (1993) 899–902.
14. D. M. Small, *Handbook of Lipid Research*, Vol. 4, Plenum Press, New York, 1986, chapters: 2, 5, 8.
15. I. Weissbuch, J. Majewski, L. Margulis, M. Lahav, and L. Leiserowitz, *J. Phys. Chem.* **97** (1993) 8692–8695.
16. D. K. Schwartz, J. Garnaes, R. Viswanathan, and J. A. N. Zasadzinski, *Science* **257** (1992) 508–511.
17. R. M. Overney, E. Meyer, J. Frommer, D. Brodbeck, R. Lüthi, L. Howald, H.-J. Güntherodt, M. Fujihira, H. Takano, and Y. Gotoh, *Nature* **359** (1992) 133–134.
18. L. F. Chi, M. Anders, H. Fuchs, R. R. Johnston, and H. Ringsdorf, *Science* **259** (1993) 213–216.
19. A. Schaper, L. Wolthaus, D. Möbius, and T. M. Jovin, *Langmuir* **9** (1993) 2178–2184.
20. J. Als-Nielsen and K. Kjaer, in: T. Riste and D. Sherrington (Eds.), *Proceedings of the Nato Advanced Study Institute,* Plenum Press, New York, Geilo, Norway, 1989, pp 113.
21. D. Jacquemain, S. Grayer Wolf, F. Leveiller, M. Deutsch, K. Kjaer, J. Als-Nielsen, M. Lahav, and L. Leiserowitz, *Angew. Chem., Int. Ed. Engl.* **31** (1992) 130–152.
22. N. Nakamura and T. Yamamoto, *Acta. Cryst.* **C50** (1994) 946–948.
23. J. L. Wang, F. Levellier, D. Jacquemain, K. Kjaer, J. Als-Nielsen, M. Lahav, and L. Leiserowitz, *J. Am. Chem. Soc.* **116** (1994) 1192–1204.
24. J. Majewski, R. Popovitz-Biro, W. G. Bowman, K. Kjaer, J. Als-Nielsen, M. Lahav, and L. Leiserowitz, *Chem.-Euro. J.* **1** (1995) 304–311.

SAŽETAK

Samoagregacija α,ω-alkandiola u dvo- i trodimenzijske kristalite na graničnoj plohi voda-zrak. Značenje za nukleaciju leda

Ronit Popovitz-Biro, Ron Edgar, Jaroslaw Majewski, Sidney Cohen, Lev Margulis, Kristian Kjaer, Jens Als-Nielsen, Leslie Leiserowitz i Meir Lahav

Pokazana je korelacija između kristalne strukture monoslojeva i multislojeva α,ω-alkandiola HO-$(CH_2)_n$-OH (n = 16, 18, 19, 21, 22, 23, 24, 30) na graničnoj plohi zrak-voda i njihove uloge kao nukleatora leda. Provedeno je određivanje strukture slijedećim metodama: difrakcijom X-zraka pri malom kutu između površine uzorka i snopa, pretražnom mikroskopijom, transmisijskom elektronskom mikroskopijom pri niskim temperaturama i FT-IR spektroskopijom.